Institutional Repository - Research Portal
Dépôt Institutionnel - Portail de la Recherche
researchportal.unamur.be
University of Namur

RESEARCH OUTPUTS / RÉSULTATS DE RECHERCHE

Cross-section measurements of the 14N(α,p)17O and 14N(α,α)14N reactions between 3.5 and 6 MeV

Terwagne, Guy; Genard, Gilles; Yedji, Mourad; Ross, Guy G.

Published in:
Journal of Applied Physics

Publication date:
2008

Document Version
Early version, also known as pre-print

Link to publication

Citation for pulished version (HARVARD):
Terwagne, G, Genard, G, Yedji, M & Ross, GG 2008, 'Cross-section measurements of the $^{14}N(\alpha,p)^{17}O$ and $^{14}N(\alpha,\alpha)^{14}N$ reactions between 3.5 and 6 MeV', *Journal of Applied Physics*, vol. 104, pp. 084909-1-8.

General rights
Copyright and moral rights for the publications made accessible in the public portal are retained by the authors and/or other copyright owners and it is a condition of accessing publications that users recognise and abide by the legal requirements associated with these rights.

- Users may download and print one copy of any publication from the public portal for the purpose of private study or research.
- You may not further distribute the material or use it for any profit-making activity or commercial gain
- You may freely distribute the URL identifying the publication in the public portal ?

Take down policy
If you believe that this document breaches copyright please contact us providing details, and we will remove access to the work immediately and investigate your claim.

Download date: 05. May. 2023

Cross-section measurements of the $^{14}N(\alpha,p)^{17}O$ and $^{14}N(\alpha,\alpha)^{14}N$ reactions between 3.5 and 6 MeV

G. Terwagne,[1,a)] G. Genard,[1] M. Yedji,[2] and G. G. Ross[2]
[1]*Centre de Recherche en Physique de la Matière et du Rayonnement, Laboratoire d'Analyses par Réactions Nucléaires, University of Namur (FUNDP), 61 Rue de Bruxelles, B-5000 Namur, Belgium*
[2]*INRS-Énergie, Matériaux et Télécommunications, 1650 Boulevard Lionel-Boulet, Varennes, Québec J3X 1S2, Canada*

(Received 11 April 2008; accepted 1 September 2008; published online 28 October 2008)

The cross-section of the $^{14}N(\alpha,p_0)^{17}O$ reaction at angles of 90°, 135°, and 165° was measured for incident energies between 3.5 and 6.0 MeV simultaneously with the cross-section of the $^{14}N(\alpha,\alpha)^{14}N$ reaction at 165°. Interference between these two reactions at the angle of 165° and around 3.9 MeV was taken into account. The technique used is very powerful, thanks to the $Ta_{450\ nm}/C$ target being implanted with a high dose of nitrogen. The $^{14}N(\alpha,p_0)^{17}O$ reaction exhibits some resonances allowing traces of nitrogen to be quantified. This reaction also offers an alternative to the $^{14}N(d,\alpha)^{12}C$ and $^{14}N(^3He,p)^{16}O$ nuclear reactions for profiling nitrogen in the first few microns below the surface. Moreover, by using α-particles, Rutherford backscattering spectroscopy can be performed simultaneously with a good mass resolution to depth profile high Z elements in the sample. The sensitivity of these reactions (0.1%) has been tested by measuring the nitrogen traces in a titanium oxide film deposited on silicon. Depth profiling of nitrogen in a TiN layer on a silicon substrate was also performed. In addition, we publish for the first time some cross-sections values for the $^{14}N(\alpha,p_1)^{17}O$ reaction at 90° and 165°; this measurement is a challenging task. © *2008 American Institute of Physics*. [DOI: 10.1063/1.3000661]

I. INTRODUCTION

Light elements such as hydrogen, carbon, nitrogen, and oxygen play an important role in the surface treatment of steels, glasses, and polymers. Protective, decorative, or adhesive coatings can be made by various techniques such as ion implantation, ion beam assisted deposition, chemical vapor deposition, and physical vapor deposition (PVD). Depth profiling of these light elements is often performed by means of resonant nuclear reaction analysis (RNRA) induced by protons or alpha particles. RNRA gives good depth resolution but only for one element at a time. Quantitative analysis and depth profiling of nitrogen are usually performed by non-resonant nuclear reaction analysis (NRA) induced by deuterons or ^{3}He particles. Although the cross-sections for (d,p) and (d,α) reactions on light elements are usually higher than those for the $(^3He,\alpha)$ or $(^3He,p)$ reactions, deuterons produce an important flux of neutrons and many laboratories are not allowed to accelerate deuterons. An alternative solution to analyze nitrogen can be the nuclear reactions induced by ^{3}He particles. The cross-sections of the $^{14}N(^3He,p)^{16}O$ and $^{14}N(^3He,\alpha)^{13}N$ reactions were measured precisely for the first time 15 years ago[1] at different angles and for energies between 1.6 and 2.8 MeV. It is worth mentioning that reactions induced by ^{3}He particles at the same energy produce 100 times fewer neutrons than (d,p) or (d,α) reactions. They are also more sensitive to the near surface since the stopping power is higher for ^{3}He than for deuterons of the same energy. However, ^{3}He gas is very expensive and most laboratories do not use such particles.

Another alternative solution to quantify nitrogen is to use reactions induced by α-particles such as $^{14}N(\alpha,\alpha)^{14}N$ and $^{14}N(\alpha,p)^{17}O$. These reactions are sensitive to the near surface and Rutherford backscattering spectroscopy (RBS) can be performed simultaneously with a good depth resolution to quantify heavy elements. For light elements, when the energy increases, the nuclear interaction between the incident α-particle and the target nucleus must by taken into account and the cross-section shows large variations in intensity due to resonances. The analysis technique is called backscattering spectroscopy (BS).

A picture of the $^{14}N(\alpha,p_0)^{17}O$ reaction in an ionization chamber was photographed in 1925 by Blackett and Lees,[2] so it was one of the first nuclear reaction to be studied even before accelerator technology. Although this reaction has a negative Q-value (−1.19 MeV), it is a good candidate for analyzing nitrogen quantitatively. Since 1958, the $^{14}N(\alpha,\alpha)^{14}N$ (Refs. 3–8) and $^{14}N(\alpha,p)^{17}O$ (Refs. 3–5 and 9–12) reactions have also been studied at various angles by different authors in the MeV energy range. The data are summarized in Table I and will be compared with our data in the result section. Discrepancies in the energy scale as well as in intensity are observed. Although the $^{14}N(\alpha,p_0)^{17}O$ reaction cross-section at $\theta_{lab}=135°$ has been measured recently,[9,12] only one measurement around $\theta_{lab}=90°$ has been done some 50 years ago by Kashy *et al.*[3] Moreover, an interference occurs between the α-particles emitted at 165° from the $^{14}N(\alpha,\alpha)^{14}N$ reaction and the protons emitted from the $^{14}N(\alpha,p_0)^{17}O$ for energies around 3.9 MeV, which is close to the 3.7 MeV resonance. To avoid this interference, we placed another particle detector at 165° relative to the incident beam

a)Electronic mail: guy.terwagne@fundp.ac.be.

 © 2008 American Institute of Physics

Author complimentary copy. Redistribution subject to AIP license or copyright, see http://jap.aip.org/jap/copyright.jsp

TABLE I. Data from the literature concerning the $^{14}N(\alpha,\alpha)^{14}N$ and $^{14}N(\alpha,p_0)^{17}O$ reactions.

Reaction	Reaction angle (Laboratory frame) (°)	E_{min} (MeV)	E_{max} (MeV)	Reference
$^{14}N(\alpha,\alpha)^{14}N$	43.1–74.1–163.5	2.7	4.9	Kashy *et al.* (Ref. 3)
$^{14}N(\alpha,\alpha)^{14}N$	75.0–109.5–114.5–167.5	2	3.8	Herring *et al.* (Ref. 4)
$^{14}N(\alpha,\alpha)^{14}N$	172	5.2	7.5	Artigalas *et al.* (Ref. 5)
$^{14}N(\alpha,\alpha)^{14}N$	167	4.5	6.5	Foster *et al.* (Ref. 6)
$^{14}N(\alpha,\alpha)^{14}N$	165	2	9	Feng *et al.* (Ref. 7)
$^{14}N(\alpha,\alpha)^{14}N$	167	5	6	Wetteland *et al.* (Ref. 3)
$^{14}N(\alpha,p_0)^{17}O$	89–163.5	3.5	4.7	Kashy *et al.* (Ref. 3)
$^{14}N(\alpha,p_0)^{17}O$	84.7–108.9–127.1–167.2	2.7	3.8	Herring *et al.* (Ref. 4)
$^{14}N(\alpha,p_0)^{17}O$	172	5.2	7.5	Artigalas *et al.* (Ref. 5)
$^{14}N(\alpha,p_0)^{17}O$	135	4	5	Giorginis *et al.* (Ref. 9)
$^{14}N(\alpha,p_0)^{17}O$	165	5.5	7.5	Xu *et al.* (Ref. 10)
$^{14}N(\alpha,p_0)^{17}O$	172	4.9	6.3	Mea *et al.* (Ref. 11)
$^{14}N(\alpha,p_0)^{17}O$	135	3.2	4	Wei *et al.* (Ref. 12)

with a 3 μm absorber foil. The energy loss by α-particles in the foil is greater than the energy loss for protons and the interference disappears. It is important to note that what we call here the 3.7 MeV resonance is actually a peak due to the presence of different resonances that are not resolved (3.67 and 3.72 MeV). It is almost the case for the other so-called resonances in the following parts.

In this paper, we will measure the $^{14}N(\alpha,\alpha)^{14}N$ and the $^{14}N(\alpha,p_i)^{17}O$ $(i=0,1)$ cross-sections over a wide range of energies (3.5–6.0 MeV) at different angles (90°, 135°, and 165°) by using a standard thin coating of Ta implanted with nitrogen. We will also present two applications to determine the sensitivity and the depth profiling capabilities of those reactions.

II. EXPERIMENTAL PROCEDURE

A. Standard preparation

Cross-section measurements require the use of standards containing a well-known and large amount of nitrogen. In this case, we used a TaN specimen produced by nitrogen implantation into Ta. Such a sample has all the qualities of a good standard: it is easily reproducible, it contains a large amount of nitrogen (~50 at. %), and it has long-term stability under ion beam irradiation. We did not use the standard that we suggested in a previous paper,[13] which consists of nitrogen implantation at high temperature in silicon. Although this kind of standard exhibits excellent qualities as reported in our paper,[13] it is not suitable because an interference occurs around 4 MeV from the $^{28}Si(\alpha,p_0)^{31}P$ reaction.

A pure tantalum layer (450 nm) was first deposited by PVD on a polished glassy carbon disk (20 mm diameter). Carbon was chosen as substrate in order to reduce the background under the nitrogen peak to almost zero. This increases the sensitivity of the measurements especially for the energy regions where the cross-section is very low. A thin tantalum nitride layer was produced by 120 keV $^{14}N_2^+$ implantation at room temperature and a dose of 10^{18} atoms/cm^2 in the Ta layer. Such a dose produces the ε-TaN rich nitrogen phase[15,16] and a nitrogen depth profile as a plateau, which contains around 60 at. % of nitrogen. The total amount of tantalum and the retained dose of nitrogen $(6.0\pm0.2\times10^{17}$ $^{14}N/cm^2)$ can be measured during all the excitation measurements because the lack of tantalum signal is due to the implanted nitrogen; moreover, it is well known that the elastic cross-section for Ta is still Rutherford in the considered energies. The thickness of the Ta layer was chosen to ensure optimal sensitivity of the reaction. Figure 1 shows a spectrum recorded on the TaN standard at a backward angle of 165° for 4.6 MeV α-particles, an energy region just above the resonance located at E_R=4.5 MeV. At that energy, the cross-section of the $^{14}N(\alpha,\alpha)^{14}N$ reaction is very low. It is clearly seen that the nitrogen region is almost free of background contributions so that the sensitivity is increased. We have also plotted a simulation for a thick Ta substrate (solid gray line). The low-intensity nitrogen peak would not be distinguished from the experimental background.

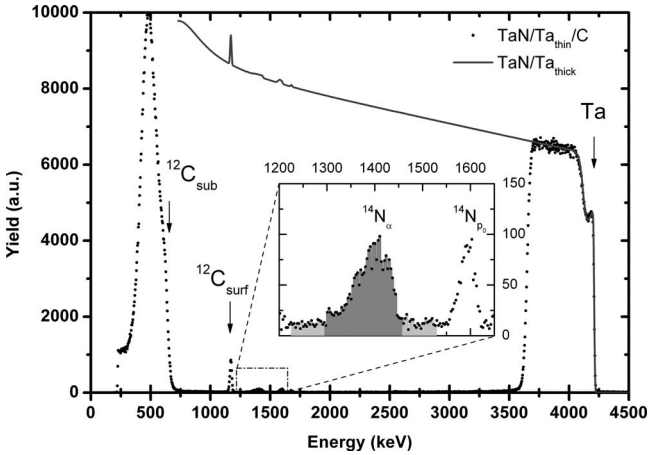

FIG. 1. Backscattering spectra for 4.6 MeV α-particles observed at 165° on TaN/Ta standards without absorber in front of the detector: experimental points on the thin Ta(^{14}N)/C standard (dots) and simulation for TaN on a thick Ta backing (solid gray line). In insert, the mean of the background on the left and right of the reaction peak is subtracted from the nitrogen peak to calculate the cross-section. $^{14}N_{\alpha}$ and $^{14}N_{p0}$ notations are for the $^{14}N(\alpha,\alpha)^{14}N$ and $^{14}N(\alpha,p_0)^{17}O$ reactions, respectively.

Author complimentary copy. Redistribution subject to AIP license or copyright, see http://jap.aip.org/jap/copyright.jsp

TABLE II. Nuclear reaction thresholds calculated using Wapstra 2003 mass evaluation (Ref. 14) and resonances used for calibrating the terminal voltage of the Tandetron accelerator. V_t and V_{exp} are the theoretical and the experimental voltages of the terminal, respectively.

Reaction	E_{th} or E_R (keV)	V_t (kV)	V_{exp} (kV)	Reaction type
$^{7}Li(p,n)^{7}Be$	1880.36	923.68	919.3	Threshold
$^{9}Be(p,n)^{9}B$	2057.24	1012.12	1006.9	Threshold
$^{11}B(p,n)^{11}C$	3017.80	1492.40	1483.3	Threshold
$^{13}C(p,n)^{13}N$	3235.48	1601.24	1593.0	Threshold
$^{15}N(p,n)^{15}O$	3774.05	1870.53	1861.4	Threshold
$^{19}F(p,\alpha\gamma)^{16}O$	340.46	153.73	153.53	Resonance
$^{19}F(p,\alpha\gamma)^{16}O$	872.11	419.56	416.87	Resonance
$^{15}F(p,\alpha\gamma)^{12}C$	429.00	198.00	197.71	Resonance

B. Accelerator energy calibration

All the measurements were done with *Accélérateur Linéaire pour l'Analyse et l'Implantation des Solides* (ALTAÏS), the 2 MV Tandetron™ accelerator installed at LARN (Namur, Belgium). In order to calibrate the voltage of the terminal, a large variety of (p,n) neutron threshold and nuclear resonant reactions induced by protons were used. These reactions, which cover the full range of accessible voltages of the tandem accelerator, are reported in Table II. The outgoing energy of the accelerated beam is given by the following formula:

$$E = (V_c + V_e + V_t)\frac{M}{M_{tot}} + qV_t, \tag{1}$$

where V_c and V_e are the cathode (30 kV) and the extraction voltages (3 kV) of the source of negative ions by cesium sputtering, respectively, V_t is the theoretical terminal voltage, M and M_{tot} are the masses of the outgoing cation and the incoming anion, respectively, and q is the charge state of the outgoing cation. Generally, the incoming anion and the outgoing cation have the same masses except for producing heavy ion beams with a very short lifetime, such as N^- for example. In Table II, the theoretical terminal voltages, V_t, calculated from formula (1) using energies calculated from the 2003 mass evaluation from Wapstra *et al.*[14] are compared with the terminal voltages actually applied, V_{exp}, for ALTAÏS. A linear regression through origin between V_t and V_{exp} gives a correlation coefficient of $R=1$. The relationship between theoretical and applied terminal voltage is given by

$$V_t = V_{exp} \times 1.0053(\pm 0.0002). \tag{2}$$

The excellent correlation means that the beam energy is not affected by the geometry of all elements included in the accelerator (source, LE acceleration and/or HE acceleration, magnet and slits). For ten years, the coefficient between V_t and V_{exp} has changed in a few 10^{-4}, which shows that solid state power supply of dynamitron is very reproducible. Nevertheless, only the voltmeter generator could affect the slope of formula (2). Resonant reactions shown in Table II are regularly used for depth profiling elements in materials, and good reproducibility is observed for the experimental voltage V_{exp}. The beam energy spread is given principally by the ripple of the high voltage terminal (~120 V), which means that the precision of the α beam energy is better than 1 keV.

C. Detection geometry

We have measured the $^{14}N(\alpha,\alpha)^{14}N$ cross-section at 165° and the $^{14}N(\alpha,p_i)^{17}O$ cross-sections (for $i=0,1$) at three different angles (90°, 135°, and 165°). Each particle detector (Planar Implanted Passivated Silicon (PIPS)) was positioned with a precision better than 0.5° for the angle. The first detector, named NRA 1, was placed 51 mm from the beam impact at 90° relative to the incident beam. A rectangular collimator (4×13 mm^2) defined a solid angle of 20.0 msr. The second detector, named NRA 2, was positioned 50 mm from the beam impact at 135° relative to the incident beam. A rectangular slit (4×13 mm^2) defined a solid angle of 20.8 msr. For both NRA detectors, Mylar™ absorber foils were placed in the path of the detected particles to stop the α-scattered particles. The thickness of the absorber foils depended on the incident energy for the excitation measurements. For energies between 3.5 and 4.5 MeV, an 18.2 μm absorber foil was sufficient to stop the scattered particles, while for energies above 4.5 MeV a thickness of 36.6 μm was necessary. A third 25 mm^2 detector (PIPS), named RBS L detector and placed 80 mm from the beam impact at backward angle (165°) and having a solid angle of 3.91 msr, was also used to measure the total amount of α-particles impinging the specimen. Finally, in order to avoid the interference between α particles emitted from the $^{14}N(\alpha,\alpha)^{14}N$ reaction and the protons emitted from the $^{14}N(\alpha,p_0)^{17}O$ reaction for energies around 3.9 MeV, we placed another particle detector at 165° relative to the incident beam with a 3 μm Mylar™ absorber foil. The energy loss by α-particles in the foil was greater than the energy loss by protons and the interference disappears. Note that another interference between $^{14}N(\alpha,p_0)^{17}O$ and $^{16}O(\alpha,\alpha)^{16}O$ around 5 MeV can also be avoided by using experimental data from this last detector.

D. Cross-section determination

The backscattering cross-section at 165° was calculated using the following expression:

$$\left(\frac{d\sigma(E)}{d\Omega}\right)_N = \frac{A_N \cos\theta_{in}}{\Omega_3 N_i (Nt)_N}, \tag{3}$$

where A_N is the area under nitrogen peak, θ_{in} is the incident angle between the incident beam and the normal of the sample ($\theta_{in}=15°$ in this case), N_i is the number of incident ions, Ω_3 is the solid angle subtended by the third detector (RBS L), $(Nt)_N$ is the number of nitrogen atoms present in the TaN layer, and E is the mean energy of the particles in the nitride layer. This mean energy is calculated assuming a homogeneous nitride layer rather than the real implanted depth profile, which is very close to a rectangular shape. Both distributions give the same results. The background under the nitrogen peak was removed by selecting the average background on the left and on the right of the peak (Fig. 1). The same relation can be written for the Rutherford cross-section for Ta

Author complimentary copy. Redistribution subject to AIP license or copyright, see http://jap.aip.org/jap/copyright.jsp

$$\left(\frac{d\sigma(\bar{E})}{d\Omega}\right)_{Ta} = \frac{A_{Ta}\cos\theta_{\text{in}}}{\Omega_3 N_i (Nt)_{Ta}}, \tag{4}$$

with the same parameters as in Eq. (3) relative to tantalum except for the energy, which is the mean energy of α-particles in the Ta coating. This approximation, which assumes that the particles have a mean energy over the entire Ta layer, leads to a negligible error estimated between 1% and 2%. The $\Omega_3 N_i$ product is determined by means of SIMNRA (Ref. 17) simulations for each different spectrum. Finally, the backscattering cross-section of α-particles from ^{14}N can be calculated by the following formula:

$$\left(\frac{d\sigma(E)}{d\Omega}\right)_N = \frac{A_N}{A_{Ta}}\frac{(Nt)_{Ta}}{(Nt)_N}\left(\frac{d\sigma(\bar{E})}{d\Omega}\right)_{Ta}, \tag{5}$$

where $(d\sigma(\bar{E})/d\Omega)_{Ta}$ is the theoretical cross-section that is in very good agreement with the experimental cross-section (less than or equal to 1% of discrepancies). For the NRA detectors, we used the same formula corrected for the solid angle ratio Ω_3/Ω_i. As we eliminate some of the main sources of uncertainties (integrated charge, solid angle), the precision on the measured cross-section is enhanced.

Carbon contamination due to buildup is regularly observed when long irradiation times are necessary, especially when cross-sections are measured over a large energy range. This phenomenon is mainly due to the residual gas in the beam line, where the vacuum is typically 10^{-4} Pa. In order to improve the statistics and obtain a good precision, the integrated charge at each energy was typically limited to 20 μC where resonances were observed and 100 μC for the plateau where the cross-section was low. We took into account the buildup of carbon by regularly measuring its content using the $^{12}C(\alpha,\alpha)^{12}C$ resonant reaction at $E_\alpha = 4.265$ MeV.[18] The evolution of carbon contamination versus integrated charge was fitted by a straight line

$$N_C = (0.150 \pm 0.006)Q, \tag{6}$$

where N_C is given in 10^{15} atoms/cm^2 and Q is the total integrated charge given in μC. The energy loss $\Delta E_{[\text{eV}]}$ in the contamination layer was then calculated by

$$\Delta E = N_c \varepsilon, \tag{7}$$

where ε is the stopping cross-section [eV/(10^{15} atoms/cm^2)]. Typical energy corrections were less than 1 keV. We have also regularly changed the position of the beam spot on the TaN standard to reduce the buildup of carbon contamination, especially where large variations in the cross-section (resonances) were encountered.

The statistical uncertainty on the nitrogen peak is estimated to be in the range of 6%–9% and the error on the nitride layer thickness does not exceed 3%. So, the total imprecision on the cross-section is typically 7%–10%. The error on the nitride layer comes from the difference between the experimental spectra and the simulation done with SIMNRA.[17] The precision of the energy provided by the Tandetron accelerator ALTAÏS and the correction made on the energy loss in the carbon contamination layer allow us to reduce the uncertainty associated with the energy to below 1 keV.

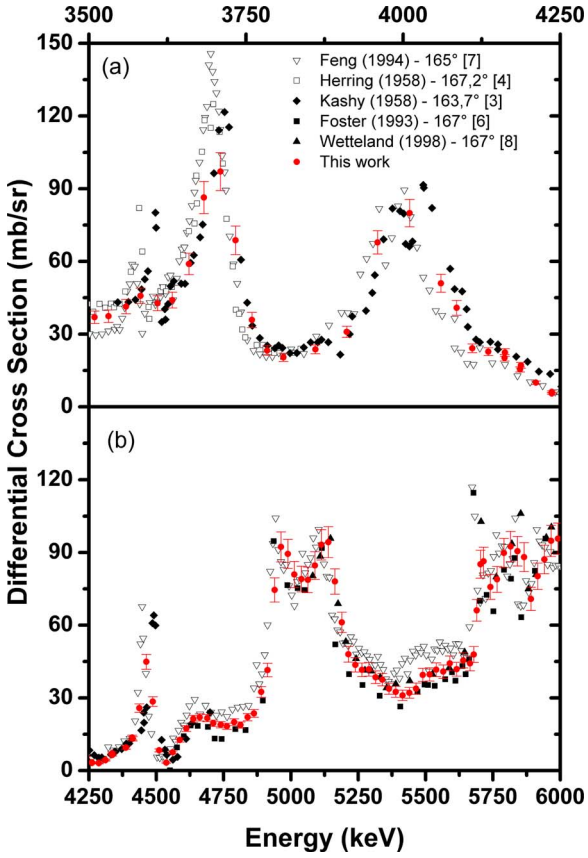

FIG. 2. (Color online) Comparison between the results obtained in this work and the data of the literature (Refs. 3, 4, and 6–8) for the $^{14}N(\alpha,\alpha)^{14}N$ reaction at 165° for energies between (a) 3.5–4.25 MeV and (b) 4.25–6.0 MeV.

III. RESULTS

Figure 2 shows the $^{14}N(\alpha,\alpha)^{14}N$ reaction cross-section at 165° for energies between 3.5 and 6.0 MeV, including the error bars. In this figure, the 3.7 MeV resonant cross-section is only for the $^{14}N(\alpha,\alpha)^{14}N$ reaction (the contribution of the $^{14}N(\alpha,p_0)^{17}O$ reaction has been subtracted). This treatment has been applied for all data for which interference between the alpha and proton peaks is observed. Those data correspond to the energies between 3.5 and 4.15 MeV. It is interesting to notice that this range is not centered on the interference energy (~3.9 MeV). This is due to the thickness of the target, which is enhanced by the straggling effect, providing a loss in resolution in the low energy part of the alpha and proton peaks.

This cross-section has to be compared with the data in the literature,[3,4,6–8] which are also reproduced in Fig. 2. The most interesting data to be compared are coming from the work of Feng *et al.*[7] that is, to the best of our knowledge, the only study that has data in the same range of energies. The values of this work are in relatively good agreement with Feng's measurements, except for energies ranging from 4.6–4.85 MeV and 5.2–5.65 MeV, where the cross-section is lower. The measurements made by Foster *et al.*[6] and Wetteland *et al.*[8] confirmed this disagreement (Fig. 2). Between

Author complimentary copy. Redistribution subject to AIP license or copyright, see http://jap.aip.org/jap/copyright.jsp

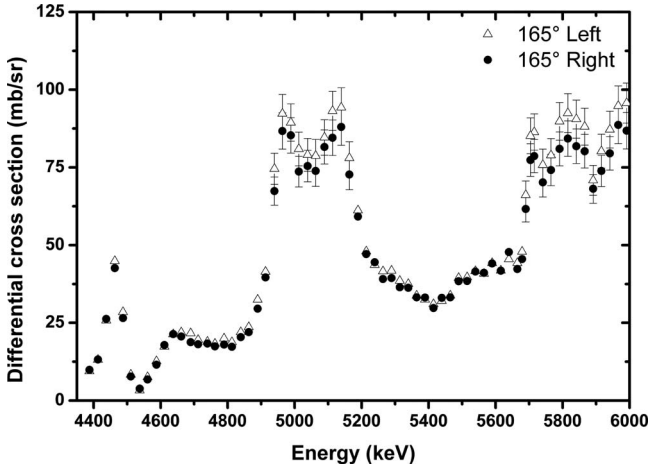

FIG. 3. Comparison between the differential cross-sections measured with the two detectors placed at 165°. The error bars are given in the regions presenting the biggest discrepancies.

4.6 and 4.85 MeV, the values of this work are between Feng and Foster ones. In the range of 5.2–5.65 MeV, our values present the same shape than Foster's but nearly the same intensity than Wetteland's. Moreover, we can see that our measurements are shifted by about 15 keV toward the higher energies. This could be important if one wants to use the 4.45 MeV resonance to probe a sample. Also, the 3.7 MeV resonance is significantly decreased by nearly 30%. This is partly due to the subtraction of the $^{14}N(\alpha,p_0)^{17}O$ contribution. Also, the energy resolution is not comparable to the ones of Feng *et al.*,[7] Herring *et al.*,[4] and Kashy *et al.*[3] due to the different targets used in the different works. Our nitrogen target is thicker (~52 keV compared with, for purpose, the ~16 keV of Feng *et al.*[7] for the energy loss of alpha particles around 3.7 MeV), which results in a mean and therefore lower value for the cross-section because the energy loss in the target can be larger than the width of some resonances. Moreover, the (α,p_0) cross-section at the interference energy (3.9 MeV) is around 3 mb/sr, which is lower than 20 mb/sr at the resonance energy. The correction is then very relevant especially if one uses an absorber in front of the detector. Nevertheless, the intensity of the cross-section above the 3.7 MeV resonance up to 3.9 MeV is in relatively good agreement with the previous measurements.

Regarding the data from the literature, a sharp resonance is seen around 3.575 MeV. This one is not really exhibited in this work, nor another one around 5.68 MeV. This is still due to the thickness of the target used, as well as for the lower intensity of the 4.45 MeV resonance. Finally, below the 3.575 MeV resonance where there are important discrepancies, the values reported here draw nearer to the ones of Herring *et al.*[4] and Kashy *et al.*,[3] contrary to the work of Feng *et al.*[7] where the 3.575 MeV resonance is also unexpectedly lower.

For energies ranging from 4.4 to 6.0 MeV, the $^{14}N(\alpha,\alpha)^{14}N$ cross-section at 165° was simultaneously measured with the two detectors placed symmetrically on the left and on the right relative to the alpha beam (Fig. 3). The results show a very good similarity, given the merging of the errors bars.

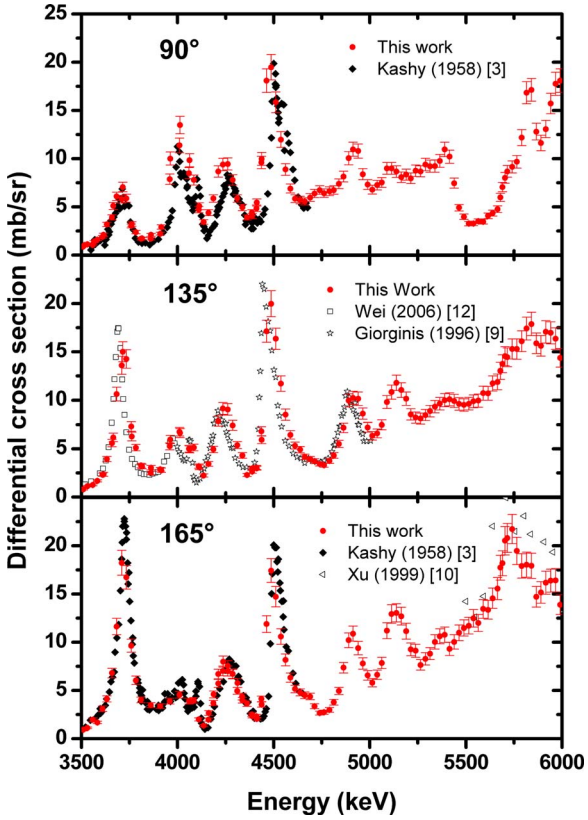

FIG. 4. (Color online) Differential cross-section of the $^{14}N(\alpha,p_0)^{17}O$ reaction at 90°, 135°, and 165° for energies between 3.5 and 6.0 MeV. The error bars are shown. Some data coming from the literature have been added for comparison (Refs. 3, 9, 10, and 12).

Concerning the $^{14}N(\alpha,p_0)^{17}O$ reaction, three different angles were investigated: 90°, 135°, and 165°. The results are shown in Fig. 4 and compared with the scanned data available in the literature.[3,9,10,12] The error bars were calculated in the same way as for the previous reaction.

At 90°, our data points are compared with the ones of Kashy *et al.*[3] The intensities are very similar but an energy shift can be observed, which is around 40 keV at the 4.5 MeV resonance. Oddly, this energy shift seems to increase with energy, which is very unusual. Nevertheless, this strange characteristic is also present for the $^{14}N(\alpha,\alpha)^{14}N$ reaction at 165° (Fig. 1), meaning that the problem does not come from our measurements. There are two references for this reaction at 135°,[9,12] allowing a comparison from 3.5 to 5.0 MeV. Again, the intensities are in very good agreement, although an energy shift is present, and our values are about 20 keV higher than the ones of Wei *et al.*[12] and Giorginis *et al.*[9] Finally, at 165°, we can compare our results with the ones of Kashy *et al.*[3] from 3.5 to 4.65 MeV. An energy shift is also observed similar to the one noted at 90°, but the intensities are very close. The data of Xu *et al.*[10] are also available from 5.5 to 6.0 MeV; these are systematically higher than our results and present also an energy shift.

Comparatively, the 3.7 MeV resonance increases substantially with the recoil angle of detected protons, as already observed by Kashy *et al.*[3] Thus, this angle of 165° is very interesting but this energy corresponds to the interference window with the $^{14}N(\alpha,\alpha)^{14}N$ reaction. So, it is necessary to

Author complimentary copy. Redistribution subject to AIP license or copyright, see http://jap.aip.org/jap/copyright.jsp

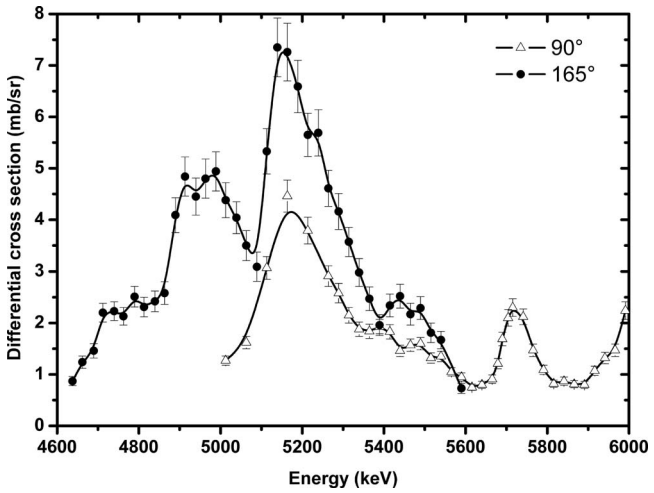

FIG. 5. (Color online) Differential cross-section of the $^{14}N(\alpha,p_1)^{17}O$ reaction at 90° and 165° for energies between 5.0–6.0 MeV and 4.65–5.6 MeV, respectively. The error bars are shown. The lines corresponding to spline connections are to guide the eyes.

work with an absorber and it is important to get a precise knowledge of the two cross-sections. This could be an alternative way to measure small quantities of nitrogen compared with the 4.5 MeV resonance for which a higher energy is required. To do this, it is necessary to place two detectors symmetrically to the incident beam: the first one as a (R)BS monitor and the second one as the NRA detector with the appropriate absorber to stop the scattered α-particles. Inversely, the resonance around 4.0 MeV decreases with the angle, while the 4.2 and 4.5 MeV resonances seem not to be angle dependant. Thanks to its large cross-section, the 4.5 MeV resonance is clearly suitable for quantifying nitrogen traces in any sample (see first application below). Finally, the 5.2 MeV resonance increases with detection angle, just as the 3.7 MeV resonance does.

At higher energies, the trend is toward a general increase in the cross-section due to the increase in the level density, although there is a high angular dependence at 90° with a slight valley around 5.5 MeV. This angle is also very interesting between 4.6 and 4.8 MeV and 5.1 and 5.35 MeV because the cross-section exhibits two plateaus with relatively high values (around 6–8 mb/sr, respectively). Those values can be used to depth profile nitrogen over several hundreds of nanometers, as illustrated in the second application below. Still at 90°, the cross-section increases to 6.0 MeV. It would be interesting to obtain measurements at higher energies to investigate whether they underline a resonance.

Finally, Fig. 5 gives some results concerning the $^{14}N(\alpha,p_1)^{17}O$ reaction cross-section, which are, to the best of our knowledge, the first published in the literature certainly because of the negative Q-value (−2.06 MeV) and the low intensity of the cross-section, as commented by Herring *et al.*[4] The error bars are shown and are a little larger than for the other cross-sections (9%–11%). Our measurements confirm that the resonance around 5.2 MeV shows the same angular evolution as the $^{14}N(\alpha,p_0)^{17}O$ reaction. This trend is observable for all energies for which the data are available. In addition to a resonance at 5.72 MeV that can be put in relation to an observable increase for the $^{14}N(\alpha,p_0)^{17}O$ reaction, the cross-section is also rising up to 6.0 MeV for this reaction. This observation gives a good reason to perform other measurements to confirm these values with the aim of simulating [with SIMNRA (Ref. 17) for instance] perfectly all contributions to an experimental spectrum.

IV. APPLICATIONS

When the energy of an α particle is increasing (>2 MeV), the minimal distance between the projectile and the target nucleus is decreasing and nuclear interaction has to be taken into account. As a consequence, diffusion cross-section decreases on heavy elements (as $1/E^2$) and the cross-section for light elements increases. Both examples given below show that trace analysis or depth profiling of light elements is possible combining (R)BS and NRA.

A. Trace analysis

A first application for this work, which illustrates its usefulness, is the characterization of a coating of TiO_2 deposited by PVD on a Si substrate in a reactive O_2 atmosphere. In this case, nitrogen traces are only due to residual vacuum before introducing a reactive gas. It is impossible to get information from the nitrogen traces in the layer with (R)BS at 165°, as the nitrogen signal cannot be distinguished from the silicon background, which shows large variations due to nuclear interactions between the projectile and the ^{28}Si nuclei. This can be overcome with a NRA detector at 90° or 135°. In this case, a detector was placed at 90° with a 24.4 μm Mylar absorber to stop the backscattered alpha particles. Figure 6 presents the (a) (R)BS and (b) NRA spectra obtained with 4.5 MeV alpha particles on the sample described above. This energy was chosen because of the 4.5 MeV resonance underlined in Fig. 4. These spectra were fitted with the SIMNRA (Ref. 17) software by using the cross-sections for nitrogen measured in this work and the cross-sections from IBANDL database for other elements [^{12}C,[18] ^{16}O,[19] and ^{28}Si (Ref. 20)]. The resonance for the $^{14}N(\alpha,p_0)^{17}O$ reaction is visible on the NRA spectrum, while the nitrogen signals ($^{14}N(\alpha,p_0)^{17}O$ and $^{14}N(\alpha,\alpha)^{14}N$) on the (R)BS spectrum are not visible. It is interesting to note that the NRA cross-sections for silicon are unknown and should be measured. The results give a layer of $Ti_{0.34}O_{0.65}N_{0.010}$, which is the TiO_2 stoechiometry with $1.0\pm0.1\%$ nitrogen. We can evaluate the sensitivity to about 0.1% nitrogen.

B. Depth profiling of nitrogen

The second application consists of carrying out a depth profile of nitrogen in the bulk of a sample. This sample is a coating of TiN deposited by PVD on a silicon substrate and was analyzed with 5.3 MeV alpha particles. Two detectors were used: one at 165° for (R)BS and another one at 90° for NRA to take advantage of the plateau in this angle-energy configuration. The two experimental spectra are given in Fig. 7 together with the theoretical fits. The amount of nitrogen was evaluated with the $^{14}N(\alpha,\alpha)^{14}N$ and $^{14}N(\alpha,p_0)^{17}O$ re-

Author complimentary copy. Redistribution subject to AIP license or copyright, see http://jap.aip.org/jap/copyright.jsp

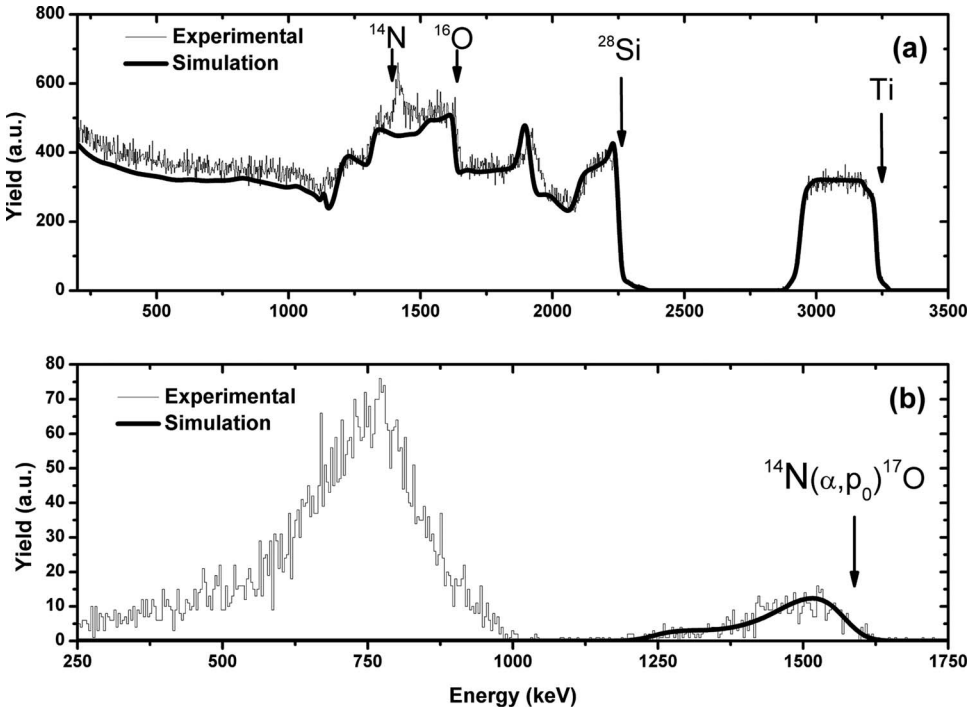

FIG. 6. Application of the cross-section measurements on TiO_2 deposited in a N_2 atmosphere on a Si substrate with 4.5 MeV α-particles. The spectra (a) (R)BS at 165° and (b) NRA at 90° obtained with an integrated charge of 40 μC during 12 min are given with the fit done by mean of SIMNRA (Ref. 17) and the cross-sections from IBANDL database (Refs. 18–20). The arrows indicate the energies of the backscattered α-particles on the elements present on the surface (except for Si). The ^{14}N contribution at the surface should appear at the corresponding arrow: it is not visible on the (R)BS spectrum but well on the NRA one.

action contributions at 165° and the $^{14}N(\alpha,p_i)^{17}O$ $(i=0,1)$ peaks at 90°. Using the cross-sections obtained in this work for nitrogen and the cross-sections from IBANDL database for other elements [^{12}C,[21] ^{16}O,[19] and ^{28}Si (Ref. 22)], we obtained a uniform layer of $Ti_{0.445}N_{0.46}C_{0.065}H_{0.03}$ of 2.35×10^{18} atoms cm^{-2} (hydrogen concentration was determined by Elastic Recoil Detection Analysis) below a hydrocarbon surface contamination. This single layer is physically correct to represent a deposition layer. Note that the energy resolution for the (α,p_0) reaction decreases to 20% due to the absorber. Here again, the silicon contribution was not well simulated in the (R)BS spectra and some nuclear reactions occurring on this element need to be taken into account at 90°.

V. CONCLUSIONS

We measured the differential cross-section of the $^{14}N(\alpha,\alpha)^{14}N$ reaction at 165° of the $^{14}N(\alpha,p_0)^{17}O$ reaction at 90°, 135°, and 165° and, for the first time, of the $^{14}N(\alpha,p_1)^{17}O$ reaction at 90° and 135°. The results have been compared with the data in the literature when available and show a good agreement. The method used is very simple and accurate, thanks to the light substrate (carbon) and the

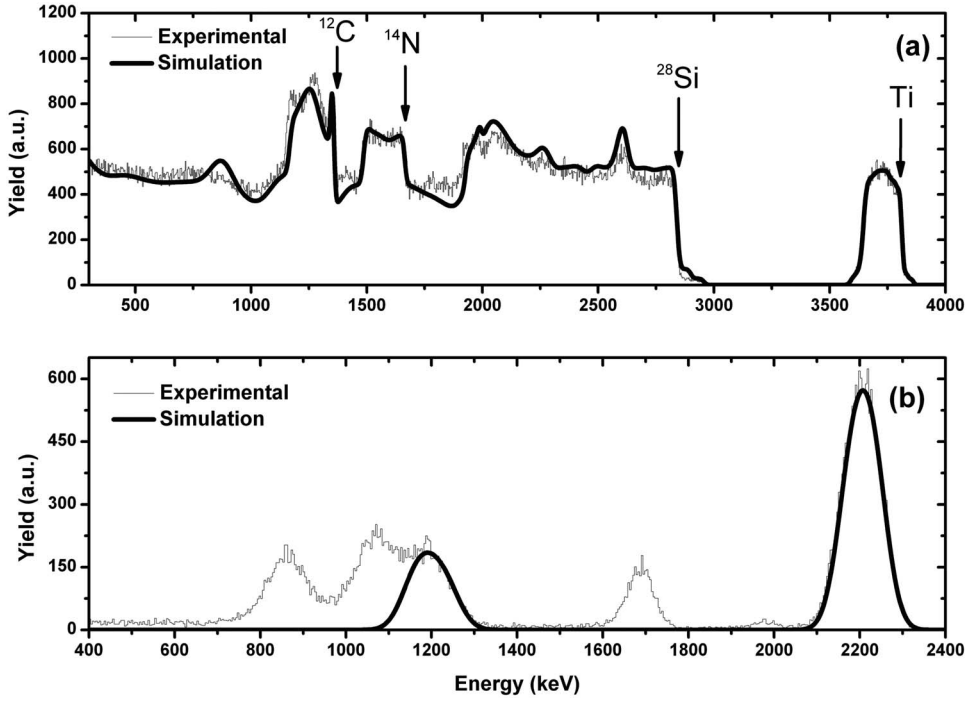

FIG. 7. Application of the cross-section measurements on a TiN layer deposited on a silicon substrate with 5.3 MeV α-particles. The spectra (a) (R)BS at 165° and (b) NRA at 90° are given with the fit done by mean of SIMNRA (Ref. 17) and the cross-sections from IBANDL database (Refs. 19, 21, and 22). The arrows indicate the energies of the backscattered α-particles on the elements present at the surface (except for Si).

Author complimentary copy. Redistribution subject to AIP license or copyright, see http://jap.aip.org/jap/copyright.jsp

heavy matrix (tantalum) that allow us to evaluate the number of the incident alpha particles and the amount of nitrogen.

The 3.7 MeV resonance for the $^{14}N(\alpha,\alpha)^{14}N$ reaction is decreased compared with the work of Feng *et al.*[7] because of the subtraction of the $^{14}N(\alpha,p_0)^{17}O$ contribution. We determined some angular evolutions for the $^{14}N(\alpha,p_i)^{17}O$ reactions $(i=0,1)$. Our results suggest that it is ideal to work at 90°. Indeed, this angle presents a plateau below 5.3 MeV that can be used to depth profile nitrogen and a high resonance at 4.5 MeV, allowing the analysis of nitrogen traces or its presence at an interface. This was applied for two different samples, demonstrating the good quality of the cross-section measurements.

ACKNOWLEDGMENTS

G.G. was supported as research fellow by the Belgian National Fund for Scientific Research (F.R.S.-FNRS) and M.Y. by the Natural Science and Engineering Research Council of Canada (NSERC). This work was realized within the SC-TEC-02 collaboration between the Wallonie-Bruxelles Community and the Québec government.

[1]G. Terwagne, D. D. Cohen, and G. A. Collins, Nucl. Instrum. Methods Phys. Res. B **84**, 415 (1994).
[2]P. M. S. Blackett and D. S. Lees, Proc. R. Soc. London, Ser. A **136**, 325 (1932).
[3]E. Kashy, P. D. Miller, and J. R. Risser, Phys. Rev. **112**, 547 (1958).
[4]D. F. Herring, R. Chiba, B. R. Gasten, and H. T. Richards, Phys. Rev. **112**, 1210 (1958).
[5]H. Artigalas, A. Chevarier, N. Chevarier, M. El Bouanani, E. Gerlic, N. Moncoffre, B. Roux, M. Stern, and J. Tousset, Nucl. Instrum. Methods Phys. Res. B **66**, 237 (1992).
[6]L. A. Foster, J. R. Tesmer, T. R. Jervis, and M. Nastasi, Nucl. Instrum. Methods Phys. Res. B **79**, 454 (1993).
[7]Y. Feng, Z. Zhou, C. Zhang, and F. Yang, Nucl. Instrum. Methods Phys. Res. B **94**, 11 (1994).
[8]C. J. Wetteland, C. J. Maggiore, J. R. Tesmer, X.-M. He, and D.-H. Lee, AIP Conf. Proc. **475**, 545 (1999).
[9]G. Giorginis, P. Misaelides, A. Crametz, and M. Conti, Nucl. Instrum. Methods Phys. Res. B **113**, 396 (1996).
[10]H. Xu, Z. Zhou, C. Zhang, G. Zhao, and L. Shi, Nucl. Instrum. Methods Phys. Res. B **149**, 390 (1999).
[11]G. D. Mea, A. Patelli, S. Restello, V. Rigato, and A. Vomiero, Nucl. Instrum. Methods Phys. Res. B **240**, 803 (2005).
[12]P. Wei, S. C. Gujrathi, M. Guihard, and F. Schiettekatte, Nucl. Instrum. Methods Phys. Res. B **249**, 85 (2006).
[13]M. Yedji, M. Bolduc, G. Genard, G. Terwagne, and G. G. Ross, Nucl. Instrum. Methods Phys. Res. B **266**, 2060 (2008).
[14]A. H. Wapstra, G. Audi, and C. Thibault, Nucl. Phys. A **729**, 129 (2003).
[15]X. Zhou, H. K. Dong, and H. D. Li, Vacuum **39**, 307 (1989).
[16]W. J. Wang, T. M. Wang, and X. J. Wang, Nucl. Instrum. Methods Phys. Res. B **108**, 300 (1996).
[17]M. Mayer, AIP Conf. Proc. **475**, 541 (1999).
[18]J. A. Leavitt, L. C. McIntyre, P. Stoss, J. G. Oder, M. D. Ashbaugh, B. Dezfouly-Arjomandy, Z. M. Yang, and Z. Lin, Nucl. Instrum. Methods Phys. Res. B **40–41**, 776 (1989).
[19]J. Demarche and G. Terwagne, J. Appl. Phys. **100**, 124909 (2006).
[20]M. K. Leung, Ph.D. thesis, University of Kentucky, 1972.
[21]Y. Feng, Z. Zhou, Y. Zhou, and G. Zhou, Nucl. Instrum. Methods Phys. Res. B **86**, 225 (1994).
[22]H.-S. Cheng, H. Shen, F. Yang, and J.-Y. Tang, Nucl. Instrum. Methods Phys. Res. B **85**, 47 (1994).

Author complimentary copy. Redistribution subject to AIP license or copyright, see http://jap.aip.org/jap/copyright.jsp